Microbes and Infection 25 (2023) 105172

Contents lists available at ScienceDirect

Microbes and Infection

journal homepage: www.elsevier.com/locate/micinf

Original article

Adhesion of human pathogenic bacteria to endothelial cells is facilitated by fibronectin interaction

Diana J. Vaca [a, 1], Fabienne Frenzel [a, 1], Wibke Ballhorn [a], Sara Garcia Torres [a], Matthias S. Leisegang [b, c], Stefan Günther [d], Daniela Bender [e], Peter Kraiczy [a], Stephan Göttig [a], Volkhard A.J. Kempf [a, *]

[a] Institute of Medical Microbiology and Infection Control, Goethe University, Paul Ehrlich Straße 40, 60596, Frankfurt, Germany
[b] Institute for Cardiovascular Physiology, Goethe University, Theodor-Stern-Kai 7, 60590, Frankfurt, Germany
[c] German Center of Cardiovascular Research (DZHK), Partner Site RheinMain, Theodor-Stern-Kai 7, 60590, Frankfurt, Germany
[d] Max Planck Institute for Heart and Lung Research, Parkstraße 1, 61231, Bad Nauheim, Germany
[e] Federal Institute for Vaccines and Biomedicines, Department of Virology, Paul Ehrlich Institute, Paul-Ehrlich-Straße 51-59, 63225, Langen, Germany

ARTICLE INFO

Article history:
Received 15 November 2022
Accepted 10 June 2023
Available online 19 June 2023

Keywords:
Endothelium
Extracellular matrix
Fibronectin
Bacterial adhesion
Bacteria-host interaction

ABSTRACT

Human pathogenic bacteria circulating in the bloodstream need to find a way to interact with endothelial cells (ECs) lining the blood vessels to infect and colonise the host. The extracellular matrix (ECM) of ECs might represent an attractive initial target for bacterial interaction, as many bacterial adhesins have reported affinities to ECM proteins, in particular to fibronectin (Fn). Here, we analysed the general role of EC-expressed Fn for bacterial adhesion. For this, we evaluated the expression levels of ECM coding genes in different ECs, revealing that Fn is the highest expressed gene and thereby, it is highly abundant in the ECM environment of ECs. The role of Fn as a mediator in bacterial cell-host adhesion was evaluated in adhesion assays of *Acinetobacter baumannii*, *Bartonella henselae*, *Borrelia burgdorferi*, and *Staphylococcus aureus* to ECs. The assays demonstrated that bacteria colocalised with Fn fibres, as observed by confocal laser scanning microscopy. Fn removal from the ECM environment (*FN1* knockout ECs) diminished bacterial adherence to ECs in both static and dynamic adhesion assays to varying extents, as evaluated via absolute quantification using qPCR. Interactions between adhesins and Fn might represent the crucial step for the adhesion of human-pathogenic Gram-negative and Gram-positive bacteria targeting the ECs as a niche of infection.

Successful infection depends on the bacterial capacity to adhere to host cells and avoid host defence or clearance systems. Host cell adhesion is the first step in infections facilitating a stable starting point on which microorganisms can colonise, replicate, persist, internalise into host compartments, and release virulence factors to enable subsequent stages of infection. The endothelium, one of the largest organ-like surfaces in the human body, consists of a single layer of endothelial cells (ECs) lining the interior surface of blood and lymphatic vessels. Because ECs and smooth muscle cells (SMCs) are two major cell types in the vasculature [1], the interaction of circulating pathogens with these cells is a likely event [2]. Infected ECs and SMCs might represent a cellular niche from which infectious pathogens can further disseminate in the human host.

ECs are cellular host targets for various bacterial infections caused by both Gram-negative and Gram-positive agents. One of the most common nosocomial pathogens, *Acinetobacter baumannii,* has been associated with bloodstream or soft tissue infections [3,4]. *Bartonella henselae,* a bacterium with a strong endothelial tropism, is responsible for, e.g., vasoproliferative tumour-like manifestations in bacillary angiomatosis and bacillary peliosis [5,6]. Dissemination and persistence of *Borrelia burgdorferi* in the human body, the causative agent of Lyme disease, have been suggested to depend on

* Corresponding author. University Hospital, Goethe University, Institute for Medical Microbiology and Infection Control, Paul-Ehrlich-Str. 40, D-60596, Frankfurt, Germany.
E-mail addresses: diana.vaca@kgu.de (D.J. Vaca), fab.frenzel@web.de (F. Frenzel), wibke.ballhorn@kgu.de (W. Ballhorn), sara.garciatorres@kgu.de (S.G. Torres), leisegang@vrc.uni-frankfurt.de (M.S. Leisegang), stefan.guenther@mpi-bn.mpg.de (S. Günther), daniela.bender@pei.de (D. Bender), kraiczy@em.uni-frankfurt.de (P. Kraiczy), stephan.goettig@kgu.de (S. Göttig), volkhard.kempf@kgu.de (V.A.J. Kempf).
[1] Equal contribution.

https://doi.org/10.1016/j.micinf.2023.105172

the bacterial ability to closely interact with blood vessels, e.g., via internalisation and induction of signalling pathways in ECs [7,8]. Moreover, infective endocarditis or septicaemic episodes caused by Gram-positive bacteria such as *Staphylococcus aureus* rely on the bacterial capacity to attach to ECs lining the heart valves and blood vessels [9,10].

The extracellular matrix (ECM) is one of the most abundant proteinaceous tissue components and provides a scaffold essential for the organisation of vascular ECs into blood vessels. The interaction between bacteria and ECM proteins [collagen, laminin, fibronectin (Fn)] has been extensively reported [11,12]. Bacterial surface proteins (i.e., adhesins) are mediators for host-cell adhesion and interaction with ECM proteins; the complexity of these adhesins ranges from monomeric proteins to intricate multimeric macromolecules. The adhesin repertoire interacting with ECM proteins in Gram-negative bacteria includes pili and non-pilus structures such as trimeric autotransporter adhesins (TAAs), other secretion systems, and lipoproteins, among others [13]. In the case of Gram-positive bacteria, a subfamily of surface proteins known as MSCRAMMs (microbial surface components recognising adhesive matrix molecules) are used to interact with ECM proteins [14]. Interaction of *A. baumannii*, *B. henselae*, *B. burgdorferi* and *S. aureus* with Fn has been widely reported using binding assays with purified Fn [15–22]. The important role of Fn binding in early infection events has been demonstrated for, e.g., *B. burgdorferi* and *S. aureus*. Here, inhibitors or antibodies blocking fibronectin resulted in lower infection rates of ECs [23,24]. To our knowledge, the relevance of Fn-mediated bacteria-host cell adhesion has been conclusively demonstrated using a cellular loss-of-function EC-adhesion model only for *B. henselae* [25].

In this work, we analysed the general role of Fn in bacterial adhesion to host cells under static and dynamic conditions for various human pathogens (*A. baumannii*, *B. henselae*, *B. burgdorferi*, and *S. aureus*). A deep understanding of the exact bacterial adhesion mechanisms to host ECs might provide opportunities for future anti-adhesion strategies to combat bacterial infections.

2. Material and methods

2.1. Bacterial strains, culture conditions, and reagents

A detailed description of bacterial strains used in this research is given in Table 1. *A. baumannii* and *S. aureus* were cultured on Columbia blood agar (CBA) plates (Thermo Fischer Scientific, Darmstadt, Germany) at 37 °C. A single colony was selected for inoculation of an overnight culture (37 °C, 180 rpm). From this, freshly prepared bacterial subcultures ($OD_{600} = 0.05$) were used for EC-adhesion experiments (until $OD_{600} = 0.2$). The number of viable *A. baumannii* and *S. aureus* was quantified from serial dilutions on CBA plates and subsequent counting of CFU units after 1 day of incubation at 37 °C.

B. henselae Marseille were cultured for three days using *Bartonella* liquid (BaLi) medium, supplemented with 2.5% Fn-depleted FCS (Sigma–Aldrich, Deisenhofen, Germany) prepared as earlier described [25]. The number of viable *B. henselae* in stock vials was quantified from serial dilutions on CBA plates and subsequent counting of colony-forming units (CFU) after 10 days of incubation at 37 °C and 5% CO_2.

B. burgdorferi were cultured until mid-log phase (5×10^7 cells/ml) at 33 °C under microaerophilic conditions in modified Barbour-Stoenner-Kelly (BSK–H) medium (Bio&SELL, Feucht, Germany). The density of spirochetes was determined using a Kova counting chamber (Hycor Biomedical, Garden Grove, CA, USA) and dark-field microscopy [26].

NEB 5 alpha competent *E. coli* (C2987H, New England Biolabs, NEB, Frankfurt, Germany; used as plasmid-harbouring standards for qPCRs) were grown overnight on solid or liquid lysogeny broth (LB; Becton Dickinson, Heidelberg, Germany).

All bacterial washing steps were performed with Dulbecco's phosphate-buffered saline no magnesium and no calcium (DPBS; Gibco, Karlsruhe, Germany). Bacteria were centrifuged at 3800×*g* for 10 min at 4 °C. Bacterial stocks (*A. baumannii*, *B. henselae*, and *S. aureus*) were stored at −80 °C in LB supplemented with 20% glycerol (VWR, Darmstadt, Germany). *B. burgdorferi* cultured in modified BSK-H medium were stored at −80 °C and used as stock cultures.

2.2. Mammalian cell culture

Human umbilical vein endothelial cells (HUVECs; C-12203, PromoCell, Heidelberg, Germany) were used for RNA-seq. Wild-type WT HUVEC (control cells expressing *FN1*) and Fn^- HUVEC (*FN1* knockout HUVEC, dual guide RNA directed lentiviral CRISPR-Cas9 targeting 5′ UTR and the intron 1 region of *FN1* gene, EC 3) [25] were used for EC-adhesion experiments and cultured using EC growth media (ECGM, C-22010, PromoCell) without antibiotics and using Fn-depleted FCS. Hep-G2 and Caco-2 cells were cultured using Dulbecco's Modified Eagle Medium (DMEM, 41,965–039, Gibco); HeLa-229 and HaCat cells were cultured using RPMI 1640 (P04-18500, PAN Biotech, Aidenbach, Germany). For all cell lines, media were supplemented with 10% FCS.

2.3. Generation of A. baumannii antibodies

Rabbit anti-*A. baumannii* IgG antibodies were prepared by using a mixture of six clinical isolates (international clusters 1,2,4,6,7, and 8) and two reference strains (ATCC 17978 and ATCC 19606). Bacteria were grown in Mueller-Hinton broth ($OD_{600} = 0.8$) and inactivated in 10% formalin for 2 h at 37 °C. Chemically-killed bacteria were used as antigen for antibody generation (Eurogentec, Seraing, Belgium).

2.4. Determination of Fn-binding to immobilised bacteria by whole-cell ELISA

Fn adherence to bacterial-coated microtiter wells was evaluated via ELISA. Bacteria were resuspended in DPBS and adjusted to the specific concentrations ($OD_{600} = 0.6$ for *A. baumannii*, *B. henselae*, and *S. aureus* correlating to ~3×10^8 cells/ml each; and 5×10^8 cells/ml for *B. burgdorferi*). Aliquots (100 μL per well) of the respective bacterial suspensions were coated onto Nunc Maxisorp flat-bottom 96-wells (468,667, Thermo Fisher Scientific) and incubated overnight at 4 °C. Plates were blocked with 3% w/v bovine serum albumin (BSA; Sigma–Aldrich) dissolved in washing buffer (0.05% v/v Tween 20 in DPBS). Increasing amounts of purified Fn (F0895, Sigma–Aldrich) were added to the wells (0, 0.2, 0.4, 0.8, 1.5, 3.0, or 6.0 μg) and incubated for 2 h at 37 °C. A subsequent step for incubation with 20% v/v rabbit serum (R4505, Sigma–Aldrich) in DPBS was added to prevent unspecific antibody binding. Interaction of bacteria with Fn was examined using mouse anti-Fn antibodies followed by horseradish peroxidase (HRP) conjugated anti-mouse IgG antibodies in blocking buffer. The reproducibility of bacteria-coated wells was confirmed using genus-specific primary antibodies and HRP-conjugated anti-mouse IgG. Antibodies and concentrations are shown in Table S1. Each step was followed by three washes using washing buffer. The assay was developed using TMB solution (T4444, Sigma–Aldrich) for 2 min. The reaction was stopped with 1 M HCl, and absorbance was measured at 450 nm

Table 1
Bacterial strains used in this study.

Bacteria	Characteristics	Reference
Acinetobacter baumannii		
ATCC 19606	type strain, isolated from the urinary tract of a patient	[58]
705	carbapenem-resistant clinical isolate (ST 2) from a patient (rectal swab)	[54]
1372	carbapenem-resistant clinical isolate (ST 2) from a patient (nose swab)	
2778	carbapenem-resistant clinical isolate (ST 2) from a patient (rectal swab)	
Bartonella henselae		
Houston-1 (ATCC49882^T var-2)	type strain, laboratory isolate (1996); variant of ATCC49882^T Houston-I	[59]
Marseille (CIP 104756)	clinical isolate from a patient diagnosed with cat scratch disease	[60]
Oklahoma (88−64)	blood isolate from a patient diagnosed with HIV (Oklahoma City, United States)	[61]
Zürich (G-5436)	human isolate, Centers for Disease Control and Prevention (Atlanta, United States); derivative of Houston-I ATCC49882^T	[62]
Borrelia burgdorferi		
B31-e2	derivative of *B. burgdorferi* type strain B31 that contains plasmids cp26, cp32-1, cp32-3, cp32-4, lp17, lp38, and lp54	[63] provided by B. Stevenson, University of Kentucky, Lexington, KY, USA
LW2	low-passage tendon isolate from a patient diagnosed with chronic Lyme borreliosis (Germany)	[64−66]
Pka-1	cerebrospinal fluid isolate from a patient diagnosed with Lyme borreliosis (Germany)	[65−67]
Staphylococcus aureus		
8325−4	laboratory strain, derivative of 8325 strain and parent strain of SH1000	[68]
NRS71	hospital-acquired clinical isolate (MRSA252), first reported in the UK; resistant to tetracycline and methicillin (ST 30)	[69]
N315	clinical isolate of a Japanese patient (pharyngeal swab). Isolated in 1982; resistant to methicillin (ST 5)	[70]
USA300	clinical isolate, first reported in the USA as cause of skin and soft tissue infection; resistant to erythromycin, methicillin, tetracycline (ST 8)	[71,72]

ST: sequence type.

using a microplate Sunrise-BasicTM reader (TECAN, Männedorf, Switzerland).

2.5. Western blotting

Mammalian cells proteins were collected using 250 μL of protein sample buffer (7 M urea, 1% SDS, 10% glycerol, 10 mM Tris−HCl pH 6.8, 5 mM DTT, all Sigma−Aldrich) containing cOmplete Protease Inhibitor Cocktail (04,693,124,001, Roche, Mannheim, Germany). Proteins (5 μg) were prepared in 6X Laemmli sample buffer. Denaturated proteins were separated by SDS-PAGE, transferred to nitrocellulose membranes, and incubated with rabbit anti-Fn and mouse anti-β-actin antibodies (overnight, 4 °C) and HRP conjugated anti-rabbit IgG or anti-mouse IgG antibodies (1 h, room temperature), respectively. For detection, blots were developed using SuperSignal West Pico PLUS Chemiluminescent Substrate (34,577, Thermo Scientific) and a Fusion FX6 EDGE Imaging System (Vilber Lourmat, Eberhardzell, Germany).

2.6. Bacterial host cell adhesion assays

HUVECs were infected, as previously described [25], with some modifications. For confocal laser scanning microscopy (CLSM), 5×10^4 cells were seeded onto collagenised coverslips in 24-well plates and were grown for 72 h without antibiotics. Adhesion experiments were performed for 60 min (*B. henselae*: MOI 100; *S. aureus*: MOI 200; *A. baumannii*: MOI 1000; *B. burgdorferi*: MOI 1000).

For static adhesion assays, 5×10^5 cells were seeded into collagenised six-well plates and grown overnight. Adhesion experiments were performed for 60 min (*B. henselae* and *S. aureus*: MOI 200; *A. baumannii* and *B. burgdorferi*: MOI 500). Before incubation, *A. baumannii* and *B. burgdorferi* were centrifuged onto HUVECs for 5 min at 300 g [27]. After adhesion, cells were washed three times with ECGM to remove unbound bacteria. For dynamic adhesion assays under shear stress conditions, 2×10^5 cells were seeded into collagenised μ-Slide I $^{0.4}$ Luer channel (Ibidi GMBH, Gräfelfing, Germany) and cultured overnight. Steril 10 or 20 ml syringes (14.85 or 19.20 mm diameter) containing pre-warmed ECGM basal and bacteria were connected to a syringe pump (KD Scientific KDS 220, Massachusetts, USA). A constant flow rate of 0.132 ml/min and shear stress of 0.125 dyne/cm^2 was maintained during the process. As an initial step, ECGM basal medium was flushed for 5 min to remove dead cells, followed by bacteria resuspended in ECGM basal medium for 40 min (*B. henselae* and *S. aureus*: MOI 200; *A. baumannii* and *B. burgdorferi*: MOI 500), and a final step with ECGM basal medium for 10 min to remove floating bacteria.

2.7. Immunofluorescence and confocal microscopy

HUVECs were fixed using 3.75% paraformaldehyde (PFA) for 10 min at 4 °C and permeabilised with 0.2% Triton X 100 for 15 min. After blocking with 1% BSA for 1 h, cells were incubated at room temperature for 1 h using various primary antibodies (rabbit anti-*A. baumannii*, rabbit anti-*B. henselae*, rabbit anti-*B. burgdorferi*, rabbit anti-*S. aureus*, mouse anti-cellular Fn, mouse anti-Fn, Alexa 488-conjugated rabbit anti-laminin, Alexa 647 conjugated rabbit anti-collagen V) and subsequently with secondary IgG-antibodies (Alexa 488 conjugated anti-rabbit IgG, Alexa 647 conjugated anti-mouse IgG). Actin cytoskeleton was stained with Alexa 555 phalloidin. Bacterial and mammalian DNA was stained with 4′,6-diamidino-2-phenylindole (DAPI) for 10 min. Antibodies and dye concentrations are shown in Table S1. Three washes with DPBS were performed between each step. Coverslips were mounted using fluorescence mounting medium (S3023, Dako, Hamburg, Germany). Slides were examined for immunofluorescence microscopy (IMF) using a Zeiss Axio Imager 2 microscope (Zeiss, Oberkochen, Germany) equipped with a Spot RT3 microscope camera (Diagnostic Instruments Inc., MI, USA) and operated by VisiView V.2.0.5 (Visitron Systems, Puchheim, Germany). Slides for confocal laser scanning microscopy (CLSM) were analysed using a Stellaris 8 System equipped with a white light laser (Leica, Mannheim,

Germany). Samples were captured using a 63x objective (HC PL APO 63×/1.3 Glyc STED WHITE) at an excitation and emission wavelength of 499 nm and 530−575 nm, respectively. Image acquisition and analysis was performed using Las X software (v4.4.0).

2.8. qPCR quantification of endothelial cell-adherent bacteria

Bacteria adherent to HUVECs were quantified by the numbers of gene copy equivalents. For static adhesion assays, cells were removed using a cell scraper, transferred to microtubes, and washed once with DPBS. For dynamic adhesion assays, ECGM basal medium was removed, and lysis buffer was added directly to flow chambers. DNA extraction was performed using alkaline lysis and neutralisation buffers as described before [25]. Amplification of species-specific genes was used to determine the bacterial and HUVECs gene copy numbers [27]. The number of adherent bacteria was quantified using a *glyA* fragment for *B. henselae* (serine hydroxymethyltransferase, 120 bp), a *rpoB* fragment for *A. baumannii* (β subunit of bacterial RNA polymerase, 110 bp) and for *S. aureus* (123 bp), and a 16 S ribosomal RNA gene fragment for *B. burgdorferi* (107 bp). The number of HUVECs was determined using a *hmbs* fragment (hydroxymethylbilane synthase, 207 bp). For each gene, a standard control was produced by ligating the PCR product into a pCR 2.1-TOPO vector (Table 2) following the manufacturer's recommendations and electroporated in NEB 5 alpha competent *E. coli*. DNA was amplified using Luna® Universal qPCR Master Mix (M3003, NEB) and 0.5 μM forward and reverse primers (Table 2). The copy numbers were calculated using the standard plasmids and molecular mass as described [25]. Absolute quantification of adherent bacteria per HUVEC was estimated using the following formula:

$$binding\ ratio = \frac{bacterial\ gene\ equivalent}{0.5\ hmbs\ gene\ equivalent}$$

2.9. RNA-Seq library preparation and analysis

Total RNA isolation of HUVEC was performed with the RNA Mini Kit (Bio&Sell, Feucht, Germany) according to the manufacturer's protocol. Total RNA and library integrity were verified on LabChip Gx Touch 24 (PerkinElmer, Massachusetts, USA). 1 μg of total RNA was used as input for SMARTer Stranded Total RNA Sample Prep Kit - HI Mammalian (Takara, Shiga, Japan). Sequencing was performed on the NextSeq 500 instrument (Illumina, Berlin, Germany) using v2 chemistry with 1 × 75bp single end setup.

Trimmomatic version 0.39 was employed to trim reads after a quality drop below a mean of Q20 in a window of 20 nucleotides and keeping only filtered reads longer than 15 nucleotides [28]. Reads were aligned versus Ensembl human genome version hg38 (Ensembl release 104) with STAR 2.7.10a [29]. Aligned reads were filtered to remove duplicates with Picard 2.25.5 (Picard: A set of tools (in Java) for working with next-generation sequencing data in the BAM format [30]) to avoid PCR artefacts leading to multiple copies of the same original fragment. Gene counts were established with featureCounts 2.0.2 by aggregating reads overlapping exons on the correct strand excluding those overlapping multiple genes [31]. The raw count matrix was normalised with DESeq2 version 1.30.1 [32]. The Ensemble annotation was enriched with UniProt data. All downstream analyses are based on the normalised gene count matrix. A global clustering heatmap of samples was created based on the euclidean distance of regularised log transformed gene counts.

2.10. Gene expression analysis using FANTOM5 data

To compare the individual gene expression towards all other cell types or tissues, each cell type-specific signal obtained with FANTOM5 Cap Analysis of Gene Expression (CAGE) was divided through the mean signal observed in all cell types or tissues and plotted. FANTOM5 CAGE expression data was obtained from the FANTOM5 website (https://fantom.gsc.riken.jp/) using the ZENBU browser (Human hg19 promoterome with gene expression). Values were taken from the track “FANTOM5 CAGE phase 1 and 2 human tracks pooled filtered with three or more tags per library and rle normalised (mean) rle” [33].

2.11. Data availability

The RNA-Seq dataset has been deposited and is available at NCBI GEO with the accession number GSE201851: https://www.ncbi.nlm.nih.gov/geo/query/acc.cgi?acc=GSE201851. The following secure token has been created to allow review of record GSE201851 while it remains in private status: ynixkqoejzqlpoj.

Table 2
Oligonucleotides and plasmids used in this study.

Plasmids	Characteristics	References
pCR 2.1-TOPO vector	standard cloning vector for TA-overhangs. Kan^r & Amp^r	Invitrogen
pCR 2.1-TOPO_*glyA*	pCR 2.1-TOPO with the *glyA* fragment from *B. henselae* Marseille	[15]
pCR 2.1-TOPO_*rpoB* (Ab)	pCR 2.1-TOPO with the *rpoB* fragment from *A. baumannii* ATCC 19606	This study
pCR 2.1-TOPO_*rpoB*(Sa)	pCR 2.1-TOPO with the *rpoB* fragment from *S. aureus* 8325-4	This study
pCR 2.1-TOPO_16 S *rDNA*	pCR 2.1-TOPO with the 16 S *rDNA* fragment from *B. burgdorferi* B31-e2	This study
pCR 2.1-TOPO_*hmbs*	pCR 2.1-TOPO with the *hmbs* fragment from HUVEC cells. Kan^r & Amp^r	[15]
PCR primers for DNA quantification	**Oligonucleotide**	**Sequence (5′-3′)**
B. henselae	*glyA*_fwd	GAC AGG AAA ATG TGC CGA AT
	*glyA*_rev	GCA GGT GAA CCA AGA CGA AT
A. baumannii	*rpoB* (Ab)_fwd	GAG TCT AAT GGC GGT GGT TC
	rpoB (Ab)_rev	ATT GCT TCA TCT GCT GGT TG
S. aureus	*rpoB*(Sa)_fwd	TGC GAA CAT GCA ACG TCA AG
	rpoB(Sa)_rev	CGA CCT CTG TGC TTA GCT GT
B. burgdorferi	16 S_fwd	GCT TCG CTT GTA GAT GAG TCT GC
	16 S_rev	TTC CAG TGT GAC CGT TCA CC
HUVEC	*hmbs*_fwd	TTC CTT CCC TGA AGG GAT TCA CTC AG
	*hmbs*_rev	TTA AGC CCA GCA GCC TAT CTG ACA CCC

2.12. Data analysis and statistics

The number of replicates is indicated in each figure. For immunofluorescence and confocal microscopy, representative pictures from at least 25 high-power fields are depicted. All statistical analyses were performed using GraphPad Prism V6 (GraphPad, San Diego, CA, USA). A value of $p < 0.05$ was considered statistically significant.

3. Results

3.1. Endothelial and smooth muscle cells predominantly express *FN1*

First, we analysed the basal endothelial gene expression of ECM components of ECs and SMC from various vessels. Individual gene expression signals were obtained from the FANTOM5 CAGE database, and the mean signal was plotted using a heat map (Fig. 1A). This analysis demonstrated that even though ECs and SMCs are functionally and phenotypically heterogeneous with marked differences in gene expression [34,35], the expression of ECM genes shows a similar pattern in both ECs and SMCs, which differs strongly from that of, e.g. adipocytes.

An RNA-seq analysis for levels of mRNA expression in HUVEC revealed that *FN1* is the highest expressed gene among the other ECM proteins (Fig. 1B) and that *FN1* expression was localised in the 20 genes most abundantly expressed in HUVECs (Table 3). Furthermore, the levels of Fn protein in HUVEC and other cells (epithelial HaCaT, Hep-G2, Caco-2, HeLa-229) were compared using the relative signal intensity of Fn bands normalised to β-actin (loading control). A predominant presence of Fn was demonstrated for HUVECs, whereas the protein levels of all other cells (quantified by the Fn/β-actin ratio) were much lower (Fig. 1C).

As (i) HUVECs are commonly used as a host cell model for infection [2], (ii) their *FN1* expression level is high, (iii) and Fn-binding proteins are present in many human pathogenic bacteria, we next analysed the role of Fn presence on ECs in the course of bacterial-EC adhesion.

3.2. Bacteria colocalise with Fn fibres of endothelial cells and interact with Fn in a dose-dependent manner

To analyse the interaction between human pathogenic bacteria and Fn in the context of host cell adhesion, confocal laser scanning microscopy (CLSM) was applied. This method allows visualising single Fn fibres on the surface of ECs and Fn-colocalising bacteria. HUVECs were infected with *A. baumannii*, *B. henselae*, *B. burgdorferi*, and *S. aureus*. These bacteria were chosen due to their described association with ECs and their already-known adhesins targeting ECM proteins [13,36]. For these assays, type strains or their derivate

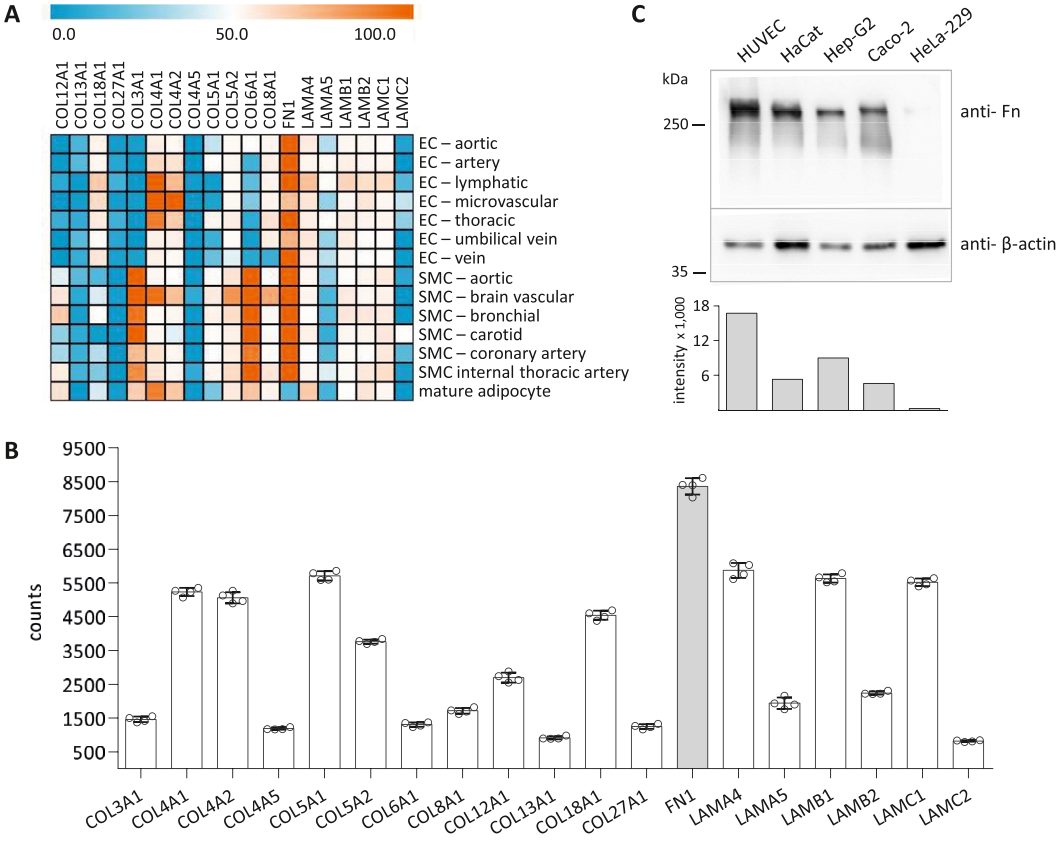

Fig. 1. Extracellular matrix (ECM) gene expression and Fn protein levels in various human cells or cell lines. (A) Heat map showing gene expression signals obtained from FANTOM5 capped analysis of gene expression (CAGE) for different collagens (*COL*), laminins (*LAM*), and fibronectin (*FN1*) across endothelial cells (EC) and smooth muscle cells (SMC) originated from different human tissues. Mature adipocytes (*FN1* low-expression) served as a reference cell type. Mean signals from different donors are shown colour-coded (blue: low expression; orange: high expression). **(B)** RNA-Seq number of read counts of extracellular matrix (ECM) genes in human umbilical vein endothelial cells (HUVECs). The number of reads mapped to each particular gene (counts) is represented as the mean of four replicates ± SD. **(C)** Analysis of Fn protein levels via Western blotting in HUVECs and epithelial cells (HaCat: human keratinocytes, Hep-G2: human liver carcinoma cells, Caco-2: human colon adenocarcinoma cells, HeLa-229: human cervix carcinoma cells). Relative signal intensity of protein bands normalised to β-actin (loading control) are depicted.

Table 3
List of the 20 highest expressed protein-coding genes in HUVECs.

Gene name	Protein description (UniProt)	Chr	Mean read counts
MACF1	microtubule-actin cross-linking factor 1	1	16,212.8
HSPG2	basement membrane-specific heparan sulfate proteoglycan core protein	1	13,855.5
DST	dystonin	6	11,114.0
AHNAK	neuroblast differentiation-associated protein AHNAK	11	10,166.0
PLEC	Plectin	8	8909.3
DYNC1H1	cytoplasmic dynein 1 heavy chain 1	14	8688.3
FN1	**fibronectin**	**2**	**8360.3**
FLNB	filamin-B	3	8273.0
MAP1B	microtubule-associated protein 1 B	5	8116.5
UTRN	utrophin	6	8015.3
HHIP	hedgehog-interacting protein	4	7607.8
FLNA	filamin-A	X	7476.8
THBS1	thrombospondin-1	15	7436.3
VWF	von Willebrand factor	12	7346.8
HUWE1	E3 ubiquitin-protein ligase HUWE1	X	7311.0
SPTBN1	spectrin beta chain, non-erythrocytic 1	2	7135.3
BMPR2	bone morphogenetic protein receptor type-2	2	6814.0
TCF4	transcription factor 4	18	6601.8
MYH9	myosin-9	22	6291.0
PRKDC	DNA-dependent protein kinase catalytic subunit	8	6224.8

strains (see Material and Methods) were used as they are widely available for reproducibility. In the case of *A. baumannii*, a multidrug-resistant patient isolate 1372, belonging to the world-wide most prevalent clonal lineage cluster 2 [37], was used instead of the type strain (ATCC 19606) because of the reduced virulence and invasion events associated with 19,606 [38]. Bacteria and Fn fibres colocalised on the endothelial surface, which was evident in XY- and XZ-sections of the infected cell layers where bacteria seem to be "captured on and in-between" Fn fibres (Fig. 2A).

To study whether the interaction of human pathogenic bacteria with Fn is a common principle in bacterial adhesion, we analysed the interaction of bacteria from different genera with Fn (purified from plasma) in binding assays using a whole-cell ELISA. Bacterial-coated wells were exposed to increasing concentrations of purified Fn, and bacterial-bond Fn was detected using anti-Fn antibodies (Fig. 2B). The results demonstrated a dose-dependent interaction between all bacteria tested herein and Fn, with the lowest binding for *A. baumannii* 1372 and the highest binding for *B. henselae* Marseille.

3.3. Bacterial host cell adhesion is facilitated by Fn interaction

To evaluate the role of cellular Fn on bacteria adhesion to ECs, we compared bacterial adhesion under static and dynamic infection conditions. For this purpose, *FN1* knockout HUVECs generated by CRISPR/Cas9 (Fn^- HUVEC) or WT HUVECs (control HUVEC, expressing *FN1*) were used, and bacterial adherence was quantified by qPCR (absolute quantification) (Fig. 3).

For analysing bacterial adhesion under static conditions (60 min), reference strains and clinical isolates were included to compare the Fn-dependent EC-binding capacity of bacteria (Fig. 3A). In case of *A. baumannii*, *B. henselae* and *S. aureus*, large differences were observed in EC-binding between reference strains and clinical isolates, whereas this was not such prominent for *B. burgdorferi*. However, a tendency of lower bacterial binding in the absence of Fn was identified for all bacteria, and a statistically significant reduction of the number of adherent bacteria detected on Fn^-HUVEC compared to control HUVEC was determined for 12/15 bacterial strains.

Furthermore, we evaluated the influence of Fn on ECs for bacterial adherence under dynamic shear stress conditions. Considering the cellular role of Fn as a scaffold for other ECM components [39], moderate shear stress (0.125 dyne/cm^2) was applied during adhesion assays (40 min) to preserve the HUVEC monolayer. Reference strains and clinical isolates with high endothelial binding (see Fig. 3A) were selected for further testing under dynamic conditions (Fig. 3B). The number of adherent bacteria detected in Fn^- HUVEC was tended to be reduced for all bacterial genera tested compared to control HUVEC (*A. baumannii* 19,606: −8%; *B. henselae* Marseille: −8%, *B. burgdorferi* B31e2: −24%, *S. aureus* USA300*:* −64%); however, only *S. aureus* exhibited a statistically significant reduction in bacterial adherence.

As many bacterial adhesins interact with other ECM proteins and Fn acts as a scaffold for the deposition of other ECM proteins, we compared the ECM proteins arrangement in control HUVEC and Fn^- HUVEC [25]. The IFM analysis of collagen V and laminin revealed the presence of both proteins unaffected in both cell types (Fig. 1S), indicating that bacterial binding reduction is correlated to Fn absence but not to other ECM components.

4. Discussion

Blood-borne infection-causing agents enter and exit through the endothelium to access and infect other tissue layers or organs (e.g., soft tissue, brain, lymph nodes). Based on the broad description of bacterial adhesins with reported affinities to ECM components, targeting the ECM protein layer on the ECs for adhesion might be a plausible strategy to support colonisation and avoid clearance [13,36]. Yet, efforts to clarify the relevance of the interactions between adhesins and ECM proteins have been focused on loss-of-function assays deleting the particular bacterial adhesin. However, analysing the role of Fn in supporting bacterial adhesion to host cells in a "bridging-like"-manner needs further scientific efforts.

Our analysis of ECM gene expression signals in different ECs and SMCs revealed that the *FN1* gene is highly expressed in both cell types responsible for the architecture of blood vessels (Fig. 1 A). An analysis of HUVECs, an infection model commonly used in bacterial adhesion research [2], revealed a predominant expression of *FN1* among all ECM genes (Fig. 1 B and Table 3), congruently with its importance for supporting vessel structure [40]. The abundance of Fn in the ECM environment conceptually makes it an interesting target for bacterial adherence *per se*, and this was observed in our experiments of infected ECs demonstrating bacteria colocalisation

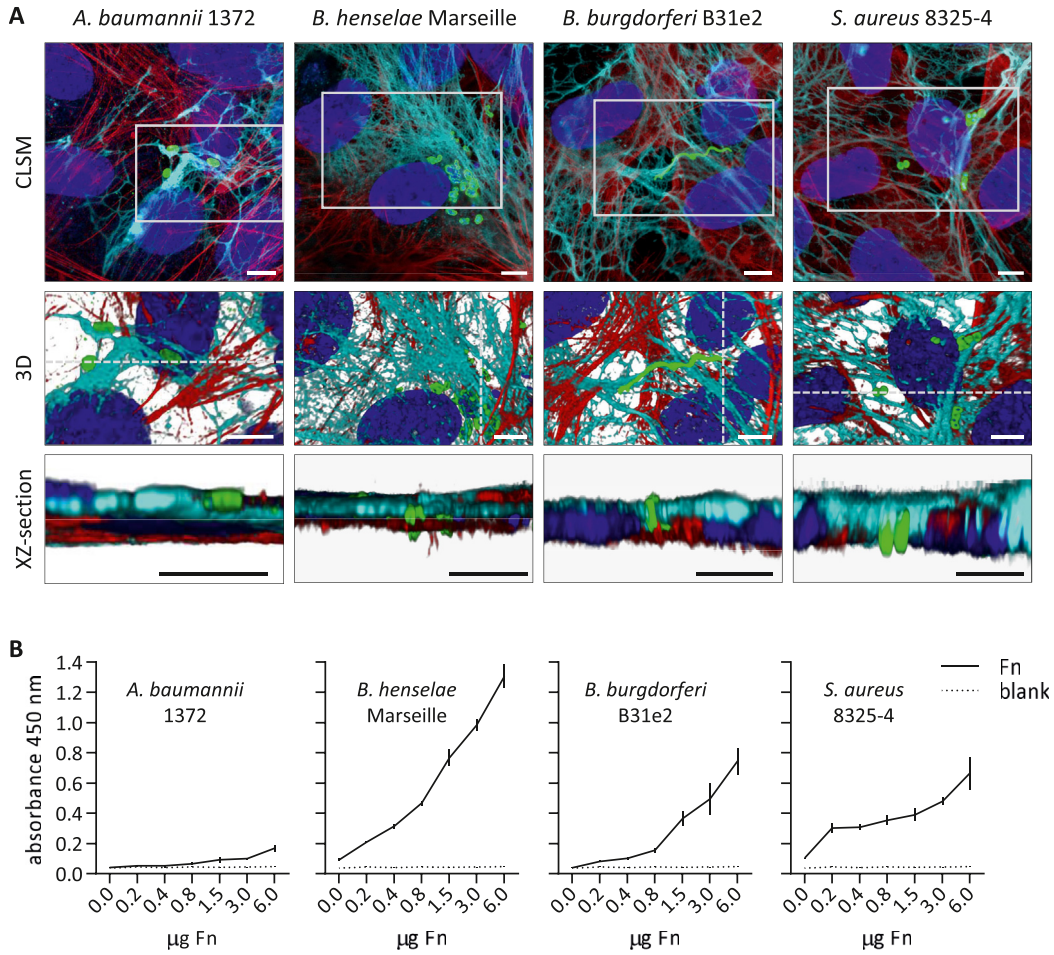

Fig. 2. Bacterial adherence to fibronectin (Fn) deposited on endothelial cells (HUVECs) surface and Fn-coated wells. **(A)** Bacterial adherence to cellular Fn deposited on the cell surface of HUVECs. Cells were infected with different bacterial genera and bacterial adhesion was analysed using confocal laser scanning microscopy (CLSM). Projection of 3D images (insert) and XZ-sections (dotted line) show close interaction between bacteria and cellular Fn (bacteria: green, nuclei: blue, beta-actin: red, Fn: cyan). Scale bar: 5 µm. **(B)** Determination of Fn-binding to immobilised bacteria by whole-cell ELISA. Microtiter wells were coated with bacteria and exposed to increased concentrations of Fn. For control, bacteria were omitted (blank). Bound Fn was detected using mouse anti-Fn antibodies. Bacterial adherence to the plates was controlled in parallel using specific bacterial antibodies (not shown).

with Fn fibres and bacterial interaction with Fn in a dose-dependent manner (Fig. 2). Based on this, we hypothesised that Fn might be a crucial mediator for bacterial adhesion. Therefore, we further evaluated the role of Fn in bacterial adhesion in loss of function experiments by removal of the possible host target using *FN1* knockout ECs [25].

Using reference strains and clinical isolates, we confirmed that Fn mediates the adhesion of Gram-negative (*A. baumannii*, *B. henselae*) and Gram-positive (*S. aureus*) bacteria as well as spirochaetes (*B. burgdorferi*) to ECs (Fig. 3). Bacterial adhesion to *FN1* knockout ECs was drastically reduced for many *B. henselae* and all *S. aureus* strains tested (Fig. 3 A). It is known for *B. henselae* that bacterial adherence to ECs and ECM proteins is mediated by the TAA protein *Bartonella* adhesin A (BadA) [17]. Furthermore, recent research described the underlying BadA–Fn interactions (on amino acid level) and also assigned Fn binding to particular BadA domains; these interactions proved to be essential for *B. henselae* adherence to ECs [25,41]. The significant role of Fn in *B. henselae* adherence was again confirmed here using *FN1* knockout ECs with a different knockout strategy. The varying EC-adhesion rates of *B. henselae* strains are most likely associated with the differences in length and domain composition of the individual BadA proteins of each particular strain [42]. In the case of *S. aureus*, the adhesins "fibronectin-binding proteins A and B" (FnBPA and FnBPB) have been described as crucial for Fn binding and for *S. aureus* internalisation into ECs [43]. Different isotypes of FnBPA and FnBPB in strain types might be responsible for variation in EC-adhesion of *S. aureus* strains [44]. Moreover, strains 8325–4, N315 and USA300 belong to the same phylogenetic group described by multilocus sequence typing [44,45]. For both species, *B. henselae* and *S. aureus*, disruption of Fn-mediated interaction certainly impacts bacterial adhesion to host cells and would represent a potentially promising target to interfere to prevent bacterial adhesion to the host.

In the case of the other Gram-negative bacteria or spirochetes, Fn-mediated adhesion might also represent an important bacterial adherence strategy supported by additional host cell receptors. For *B. burgdorferi* and *A. baumannii,* our results demonstrated that adhesion to Fn-deficient ECs was reduced but not significantly for all the strains (Fig. 3 A). It is known that adhesion of *B. burgdorferi* to ECs is mediated by the interaction of various adhesins and host receptors [46]. *Borrelia* proteins involved in adherence such as BBK32, OspC, CspA, CspZ, BB0347, RevA and RevB have reported binding affinities to Fn, and, in addition, BBK32 has proven to be crucial for bacterial stabilisation on ECs [20,47–50]. Nevertheless,

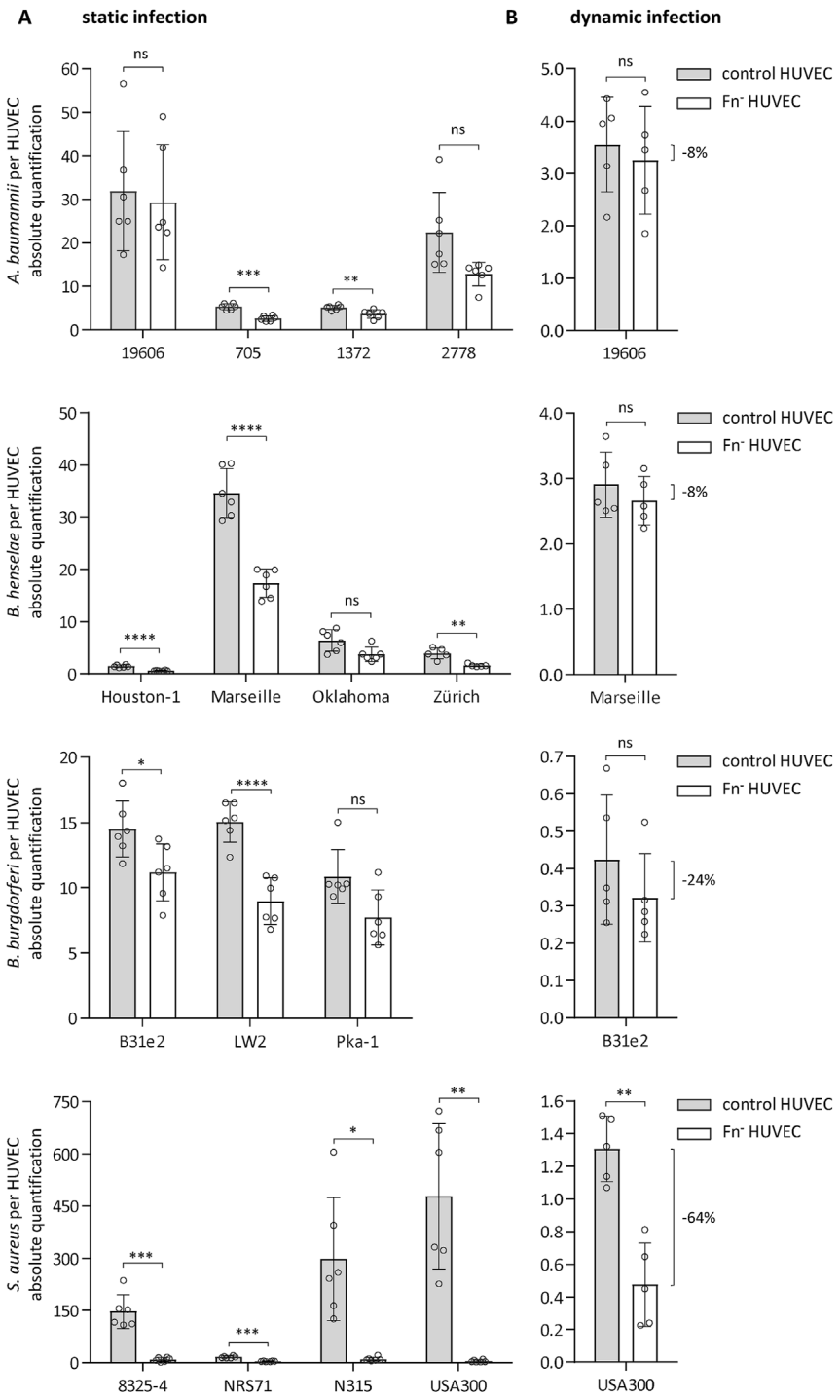

Fig. 3. Bacterial adherence to *FN1*-expressing and *FN1* knockout endothelial cells (HUVECs). Bacteria were evaluated for their adhesion capacity to control HUVEC (expressing *FN1*) and Fn$^-$ HUVEC (*FN1* knockout). Bacterial adherence was evaluated via qPCR by absolute quantification of HUVEC-bound bacteria [bacteria: housekeeping gene equivalents (*A. baumannii*: *rpoB*, *B. henselae*: *glyA*, *B. burgdorferi*: 16 S *rDNA*, and *S. aureus*: *rpoB*); HUVECs: *hmbs* gene equivalents]. **(A)** For static infection, HUVECs were infected with bacteria on six-well plates for 60 min. **(B)** For dynamic infection under shear stress conditions, HUVECs were infected with bacteria in flow chambers for 40 min under constant flow conditions (shear stress 0.125 dyne/cm^2). The mean and SD of replicates are depicted. Statistical significance was determined using two-tailed paired Student's t test comparing control and Fn$^-$ HUVEC for each bacterial strain (ns: no significant; *p < 0.02; **p < 0.0099; ***p < 0.0009; ****p < 0.0001).

interactions of other *Borrelia* adhesins (e.g., BmpA-D, DbpA and DbpB, Bgp, P66, BBA33, BB0460, ErpX) and host targets (e.g., collagen, laminin, decorin) might also account for bacterial binding in the absence of Fn [51]. For *A. baumannii*, bacterial adherence to ECs was reported to be mediated via the *Acinetobacter* trimeric autotransporter (Ata) protein [52]. Ata demonstrated binding affinities to laminin and various collagens and, to a lower extent, to Fn [53], in congruence with the observed relatively low dose-dependent binding to purified Fn (Fig. 2 B). This was confirmed in our adhesion assays where Fn removal from HUVECs (Fn$^-$ HUVEC) seems to have a variable effect on EC binding of various *A. baumannii* strains (statistically significant difference only for 705

and 1372). Moreover, although all clinical isolates used herein were confirmed to express Ata (data not shown) and belong to the same clonal lineage (ST 2), variation in the binding capacity to HUVEC was observed which might be related to the expression of different virulence traits between clinical isolates [54].

The presence of adhesins equips bacteria to stabilise surface adhesion. In the vasculature, fluid shear stress is an important physiological parameter that affects the adhesion of pathogens, resulting in a lower number of adherent bacteria (Fig. 3 B). The total number of EC-adherent *A. baumannii* and *B. henselae* was higher than for *B. burgdorferi* and *S. aureus*, a fact most likely related to the presence of TAAs and their crucial role in adherence under shear stress conditions [27]. Moreover, when using Fn knockout ECs, the application of dynamic infection assays revealed a reduction in bacterial binding for all genera tested, with a more significant impact for *S. aureus*, where EC-binding is exceptionally dependent on the presence of Fn on ECs.

The scenario of bacterial adhesion to the host shows a complex interplay of multiple variables. The presence of selective adhesion mechanisms dependent on the time of infection, host cell tropism, ECM composition, and the redundancy of interaction between adhesins and cellular receptors are all aspects to consider. For instance, infections with *B. henselae* and *S. aureus* have been associated with infective endocarditis [55]. Already in 1985, it was speculated that the interaction of pathogenic bacteria with Fn correlates with the capacity to cause endocarditis and, therefore, with bacterial adherence to heart valves [56]. In the case of *B. burgdorferi* and *A. baumannii*, bacterial interaction with ECs might represent a way to reach deeper tissue, evade the host's immune response, and attain persistence, as proposed for *B. burgdorferi* invasion of ECs and its contribution to Lyme disease [7,8]. Furthermore, the stepwise interaction of bacteria with different tissue and host components might modulate bacterial adherence to their specific targets in the organism. This was observed, e.g., for binding of *B. burgdorferi* with circulating plasma Fn and the resulting stabilisation of EC interactions under vascular shear stress, perhaps by Fn−Fn interactions [47]. Finally, more selective adhesion mechanisms can be employed by bacteria under different physiological conditions, changing its adherence mechanism as observed for *A. baumannii* binding to human lung epithelial cells (A549 cells), where interaction between Fn and three OMPs (TonB-dependent copper, OmpA, and 34 kDa Omp) was crucial for epithelial adherence [15].

The herein presented results demonstrate that the interaction of Fn on ECs with Gram-positive or Gram-negative bacteria in the context of pathogen adherence might represent an important pathogenicity strategy. Fn-mediated interaction might be an important clue in infections by bacteria with endothelial tropism (*B. henselae* and *S. aureus*) and bacteria whose interaction with ECs represents an initial step for pathogen dissemination and persistence (*B. burgdorferi* and *A. baumannii*). Dissecting the molecular mechanisms involved in bacteria-ECM interactions might bring significant information regarding the complex bacterium-host interplay and provide strategies for the interference of this interaction to prevent bacterial infections by novel approaches. For the latter, such anti-virulence strategies may not necessarily target bacterial adhesins but certain canonical domains of the matrix proteins (e.g., heparin-binding domains of Fn) [57].

Author contributions

V.A.J.K. and D.J.V. designed the study. F.F., D.J.V., W·B., and P.K. performed the experimental work. S.G.T. prepared anti-*A. baumannii* antibodies. M.S.L. and S.G. performed RNA-Seq library preparation, analysis and FANTOM5 data analysis. D.B. performed the CLSM (confocal laser scanning microscopy) analysis. W.B. and P.K. helped with EC-adhesion assays. D.J.V. and V.A.J.K. wrote the manuscript. All authors approved the final manuscript.

Conflict of interest

The authors declare no competing interests.

Acknowledgements

We thank Ralf P. Brandes (Institute for Cardiovascular Physiology, Goethe University of Frankfurt, Germany) for help with the RNA-Seq data and Andreas Peschel (Infection Biology Department, University of Tübingen, Germany) for kindly providing *Staphylococcus aureus* strains. This research was supported by the Robert Koch-Institute, Berlin, Germany (Bartonella consiliary laboratory, 1369-354), by the Deutsche Forschungsgemeinschaft (DFG FOR 2251 "Adaptation and persistence of *Acinetobacter baumannii*"), by the Clusters4Future initiative of the German Federal Ministry of Education and Research (PROXIDRUGS; 03ZU1109IA) and by the LOEWE Center DRUID (Novel Drug Targets against Poverty-Related and Neglected Tropical Infectious Diseases.)

Appendix A. Supplementary data

Supplementary data to this article can be found online at https://doi.org/10.1016/j.micinf.2023.105172.

References

[1] Lilly B. We have contact: endothelial cell-smooth muscle cell interactions. Physiology 2014;29:234−41.
[2] Valbuena G, Walker DH. The endothelium as a target for infections. Annu Rev Pathol 2006;1:171−98.
[3] Guerrero DM, Perez F, Conger NG, Solomkin JS, Adams MD, Rather PN, et al. *Acinetobacter baumannii*-associated skin and soft tissue infections: recognizing a broadening spectrum of disease. Surg Infect (Larchmt) 2010;11:49−57.
[4] Chopra T, Marchaim D, Awali RA, Krishna A, Johnson P, Tansek R, et al. Epidemiology of bloodstream infections caused by *Acinetobacter baumannii* and impact of drug resistance to both carbapenems and ampicillin-sulbactam on clinical outcomes. Antimicrob Agents Chemother 2013;57:6270−5.
[5] Dehio C, Meyer M, Berger J, Schwarz H, Lanz C. Interaction of *Bartonella henselae* with endothelial cells results in bacterial aggregation on the cell surface and the subsequent engulfment and internalisation of the bacterial aggregate by a unique structure, the invasome. J Cell Sci 1997;110:2141−54.
[6] Pulliainen AT, Dehio C. Persistence of *Bartonella* spp. stealth pathogens: from subclinical infections to vasoproliferative tumor formation. FEMS Microbiol Rev 2012;36:563−99.
[7] Yuste RA, Muenkel M, Axarlis K, Gómez Benito MJ, Reuss A, Blacker G, et al. *Borrelia burgdorferi* modulates the physical forces and immunity signaling in endothelial cells. iScience 2022;25:104793.
[8] Ma Y, Sturrock A, Weis JJ. Intracellular localization of *Borrelia burgdorferi* within human endothelial cells. Infect Immun 1991;59:671−8.
[9] Que YA, Haefliger JA, Piroth L, François P, Widmer E, Entenza JM, et al. Fibrinogen and fibronectin binding cooperate for valve infection and invasion in *Staphylococcus aureus* experimental endocarditis. J Exp Med 2005;201:1627−35.
[10] Foster TJ, Geoghegan JA, Ganesh VK, Höök M. Adhesion, invasion and evasion: the many functions of the surface proteins of *Staphylococcus aureus*. Nat Rev Microbiol 2014;12:49−62.
[11] Hymes JP, Klaenhammer TR. Stuck in the middle: fibronectin-binding proteins in Gram-positive bacteria. Front Microbiol 2016;7:1504.
[12] Singh B, Fleury C, Jalalvand F, Riesbeck K. Human pathogens utilize host extracellular matrix proteins laminin and collagen for adhesion and invasion of the host. FEMS Microbiol Rev 2012;36:1122−80.
[13] Vaca DJ, Thibau A, Schütz M, Kraiczy P, Happonen L, Malmström J, et al. Interaction with the host: the role of fibronectin and extracellular matrix proteins in the adhesion of Gram-negative bacteria. Med Microbiol Immunol 2020;209:277−99.
[14] Vengadesan K, Narayana SVL. Structural biology of Gram-positive bacterial adhesins. Protein Sci 2011;20:759−72.
[15] Smani Y, McConnell MJ, Pachón J. Role of fibronectin in the adhesion of *Acinetobacter baumannii* to host cells. PLoS One 2012;7:e33073.

[16] Smani Y, Dominguez-Herrera J, Pachon J. Association of the outer membrane protein Omp33 with fitness and virulence of *Acinetobacter baumannii*. J Infect Dis 2013;208:1561–70.
[17] Riess T, Andersson SGE, Lupas A, Schaller M, Schäfer A, Kyme P, et al. *Bartonella* adhesin A mediates a proangiogenic host cell response. J Exp Med 2004;200:1267–78.
[18] Dabo SM, Confer AW, Saliki JT, Anderson BE. Binding of *Bartonella henselae* to extracellular molecules: identification of potential adhesins. Microb Pathog 2006;41:10–20.
[19] Probert WS, Johnson BJB. Identification of a 47 kDa fibronectin-binding protein expressed by *Borrelia burgdorferi* isolate B31. Mol Microbiol 1998;30:1003–15.
[20] Brissette CA, Bykowski T, Cooley AE, Bowman A, Stevenson B. *Borrelia burgdorferi* RevA antigen binds host fibronectin. Infect Immun 2009;77:2802–12.
[21] Kuusela P. Fibronectin binds to *Staphylococcus aureus*. Nature 1978;276:718–20.
[22] Geraci J, Neubauer S, Pöllath C, Hansen U, Rizzo F, Krafft C, et al. The *Staphylococcus aureus* extracellular matrix protein (Emp) has a fibrous structure and binds to different extracellular matrices. Sci Rep 2017;7:1–14.
[23] Cordero D, Fullenkamp C, Pelly R, Reed K, Caffo L, Zahrt A, et al. Small molecule inhibitors limit endothelial cell invasion by *Staphylococcus aureus*. Curr Pharmaceut Biotechnol 2014;15:727–37.
[24] Norman MU, Moriarty TJ, Dresser AR, Millen B, Kubes P, Chaconas G. Molecular mechanisms involved in vascular interactions of the Lyme disease pathogen in a living host. PLoS Pathog 2008;4:e1000169.
[25] Vaca DJ, Thibau A, Leisegang MS, Malmström J, Linke D, Eble JA, et al. Interaction of *Bartonella henselae* with fibronectin represents the molecular basis for adhesion to host cells. Microbiol Spectr 2022;10:e0059822.
[26] Hammerschmidt C, Klevenhaus Y, Koenigs A, Hallström T, Fingerle V, Skerka C, et al. BGA66 and BGA71 facilitate complement resistance of *Borrelia bavariensis* by inhibiting assembly of the membrane attack complex. Mol Microbiol 2016;99:407–24.
[27] Weidensdorfer M, Chae JI, Makobe C, Stahl J, Averhoff B, Mller UV, et al. Analysis of endothelial adherence of *Bartonella henselae* and *Acinetobacter baumannii* using a dynamic human *ex vivo* infection model. Infect Immun 2016;84:711–22.
[28] Bolger AM, Lohse M, Usadel B. Trimmomatic: a flexible trimmer for Illumina sequence data. Bioinformatics 2014;30:2114–20.
[29] Dobin A, Davis CA, Schlesinger F, Drenkow J, Zaleski C, Jha S, et al. STAR: ultrafast universal RNA-seq aligner. Bioinformatics 2013;29:15–21.
[30] Institute B. Picard toolkit. 2019. http://broadinstitute.github.io/picard.
[31] Liao Y, Smyth GK, Shi W. FeatureCounts: an efficient general purpose program for assigning sequence reads to genomic features. Bioinformatics 2014;30:923–30.
[32] Love MI, Huber W, Anders S. Moderated estimation of fold change and dispersion for RNA-seq data with DESeq2. Genome Biol 2014;15:1–21.
[33] Lizio M, Harshbarger J, Shimoji H, Severin J, Kasukawa T, Sahin S, et al. Gateways to the FANTOM5 promoter level mammalian expression atlas. Genome Biol 2015;16:22.
[34] Garlanda C, Dejana E. Heterogeneity of endothelial cells. Arterioscler Thromb Vasc Biol 1997;17:1193–202.
[35] Zhu T, Lan B, Meng L, Yang Y, Li R, Li E, et al. ECM-related gene expression profile in vascular smooth muscle cells from human saphenous vein and internal thoracic artery. J Cardiothorac Surg 2013;8:155.
[36] Hammerschmidt S, Rohde M, Preissner KT. Extracellular matrix interactions with Gram-positive pathogens. Gram-Positive Pathog 2019:108–24.
[37] Higgins PG, Dammhayn C, Hackel M, Seifert H. Global spread of carbapenem-resistant *Acinetobacter baumannii*. J Antimicrob Chemother 2010;65:233–8.
[38] Sycz G, Venanzio GD, Distel JS, Sartorio MG, Le NH, Scott NE, et al. Modern *Acinetobacter baumannii* clinical isolates replicate inside spacious vacuoles and egress from macrophages. PLoS Pathog 2021;17:1–19.
[39] Singh P, Carraher C, Schwarzbauer JE. Assembly of fibronectin extracellular matrix. Annu Rev Cell Dev Biol 2010;26:397–419.
[40] Astrof S, Hynes RO. Fibronectins in vascular morphogenesis. Angiogenesis 2009;12:165–75.
[41] Thibau A, Vaca DJ, Bagowski M, Hipp K, Bender D, Ballhorn W, et al. Adhesion of *Bartonella henselae* to fibronectin is mediated via repetitive motifs present in the stalk of *Bartonella* adhesin A. Microbiol Spectr 2022;10:e0211722.
[42] Thibau A, Hipp K, Vaca DJ, Chowdhury S, Malmström J, Saragliadis A, et al. Long-Read sequencing reveals genetic adaptation of *Bartonella* adhesin A among different *Bartonella henselae* isolates. Front Microbiol 2022;13:1–17.
[43] Speziale P, Pietrocola G. The multivalent role of Fibronectin-Binding Proteins A and B (FnBPA and FnBPB) of *Staphylococcus aureus* in host infections. Front Microbiol 2020;11:1–13.
[44] Burke FM, McCormack N, Rindi S, Speziale P, Foster TJ. Fibronectin-binding protein B variation in *Staphylococcus aureus*. BMC Microbiol 2010;10:1–15.
[45] Cooper JE, Feil EJ. The phylogeny of *Staphylococcus aureus* – which genes make the best intra-species markers? Microbiology 2006;152:1297–305.
[46] Antonara S, Ristow L, Coburn J. Adhesion mechanisms of *Borrelia burgdorferi*. The Prokaryotes 2011:35–49.
[47] Hallström T, Haupt K, Kraiczy P, Hortschansky P, Wallich R, Skerka C, et al. Complement regulator–acquiring surface protein 1 of *Borrelia burgdorferi* binds to human bone morphogenic protein 2, several extracellular matrix proteins, and plasminogen. J Infect Dis 2010;202:490–8.
[48] Ebady R, Niddam AF, Boczula AE, Kim YR, Gupta N, Tang TT, et al. Biomechanics of *Borrelia burgdorferi* vascular interactions. Cell Rep 2016;16:2593–604.
[49] Lin Y-P, Tan X, Caine JA, Castellanos M, Chaconas G, Coburn J, et al. Strain-specific joint invasion and colonization by Lyme disease spirochetes is promoted by outer surface protein C. PLoS Pathog 2020;16:e1008516.
[50] Gaultney RA, Gonzalez T, Floden AM, Brissette CA. BB0347, from the lyme disease spirochete *Borrelia burgdorferi*, is surface exposed and interacts with the CS1 heparin-binding domain of human fibronectin. PLoS One 2013;8:e75643.
[51] Coburn J, Garcia B, Hu LT, Jewett MW, Kraiczy P, Norris SJ, et al. Lyme disease pathogenesis. Curr Issues Mol Biol 2021;42:473–518.
[52] Weidensdorfer M, Ishikawa M, Hori K, Linke D, Djahanschiri B, Iruegas R, et al. The *Acinetobacter* trimeric autotransporter adhesin Ata controls key virulence traits of *Acinetobacter baumannii*. Virulence 2019;10:68–81.
[53] Bentancor LV, Camacho-Peiro A, Bozkurt-Guzel C, Pier GB, Maira-Litrán T. Identification of Ata, a multifunctional trimeric autotransporter of *Acinetobacter baumannii*. J Bacteriol 2012;194:3950–60.
[54] Leukert L, Tietgen M, Krause FF, Schultze TG, Fuhrmann DC, Debruyne C, et al. Infection of endothelial cells with *Acinetobacter baumannii* reveals remodelling of mitochondrial protein complexes. Microbiol Spectr 2023;11(3):e0517422.
[55] Obino D, Duménil G. The many faces of bacterium-endothelium interactions during systemic infections. Microbiol Spectr 2019;7:69–81.
[56] Scheld WM, Strunk RW, Balian G, Calderone RA. Microbial adhesion to fibronectin *in vitro* correlates with production of endocarditis in rabbits. Exp Biol Med 1985;180:474–82.
[57] Henderson B, Nair S, Pallas J, Williams MA. Fibronectin: a multidomain host adhesin targeted by bacterial fibronectin-binding proteins. FEMS Microbiol Rev 2011;35:147–200.
[58] Hugh R, Reese R. A comparison of 120 strains of *Bacterium anitratum* Schaub and Hauber with the type strain of this species. Int J Syst Bacteriol 1968;18:207–29.
[59] Riess T, Raddatz G, Linke D, Schäfer A, Kempf VAJ. Analysis of *Bartonella* adhesin A expression reveals differences between various *B. henselae* strains. Infect Immun 2007;75:35–43.
[60] Drancourt M, Birtles R, Raoult D, Chaumentin G, Vandenesch F, Etienne J. New serotype of *Bartonella henselae* in endocarditis and cat-scratch disease. Lancet 1996;347:441–3.
[61] Welch DF, Pickett DA, Slater LN, Steigerwalt AG, Brenner DJ. *Rochalimaea henselae* sp. nov., a cause of septicemia, bacillary angiomatosis, and parenchymal bacillary peliosis. J Clin Microbiol 1992;30:275–80.
[62] Regnery RL, Anderson BE, Clarridge JE, Rodriguez-Barradas MC, Jones DC, Carr JH. Characterization of a novel *Rochalimaea* species, *R. henselae* sp. nov., isolated from blood of a febrile, human immunodeficiency virus-positive patient. J Clin Microbiol 1992;30:265–74.
[63] Babb K, McAlister JD, Miller JC, Stevenson B. Molecular characterization of *Borrelia burgdorferi* erp promoter/operator elements. J Bacteriol 2004;186:2745–56.
[64] Häupl T, Hahn G, Rittig M, Krause A, Schoerner C, Schönherr U, et al. Persistence of *Borrelia burgdorferi* in ligamentous tissue from a patient with chronic lyme borreliosis. Arthritis Rheum 1993;36:1621–6.
[65] Kraiczy P, Hunfeld K-P, Breitner-Ruddock S, Würzner R, Acker G, Brade V. Comparison of two laboratory methods for the determination of serum resistance in *Borrelia burgdorferi* isolates. Immunobiology 2000;201:406–19.
[66] Kraiczy P, Skerka C, Brade V, Zipfel PF. Further characterization of complement regulator-acquiring surface proteins of *Borrelia burgdorferi*. Infect Immun 2001;69:7800–9.
[67] Will G, Jauris-Heipke S, Schwab E, Busch U, Rößler D, Soutschek E, et al. Sequence analysis of ospA genes shows homogeneity within *Borrelia burgdorferi* sensu stricto and *Borrelia afzelii* strains but reveals major subgroups within the *Borrelia garinii* species. Med Microbiol Immunol 1995;184:73–80.
[68] Novick R. Properties of a cryptic high-frequency transducing phage in *Staphylococcus aureus*. Virology 1967;33:155–66.
[69] Holden MTG, Feil EJ, Lindsay JA, Peacock SJ, Day NPJ, Enright MC, et al. Complete genomes of two clinical *Staphylococcus aureus* strains: evidence for the rapid evolution of virulence and drug resistance. Proc Natl Acad Sci USA 2004;101:9786–91.
[70] Kuroda M, Ohta T, Uchiyama I, Baba T, Yuzawa H, Kobayashi I, et al. Whole genome sequencing of meticillin-resistant *Staphylococcus aureus*. Lancet 2001;357:1225–40.
[71] McDougal LK, Steward CD, Killgore GE, Chaitram JM, McAllister SK, Tenover FC. Pulsed-field gel electrophoresis typing of oxacillin-resistant *Staphylococcus aureus* isolates from the United States: establishing a national database. J Clin Microbiol 2003;41:5113–20.
[72] Tenover FC, Goering RV. Methicillin-resistant *Staphylococcus aureus* strain USA300: origin and epidemiology. J Antimicrob Chemother 2009;64:441–6.